# Time-slot based architecture for power beam-assisted relay techniques in CR-WSNs with transceiver hardware inadequacies

**Mushtaq Muhammad UMER**[1,2] , **Hong JIANG**[1]* , **Qiuyun ZHANG**[1] , **Liu MANLU**[1] ,
and **Owais MUHAMMAD**[1]

[1] School of Information Engineering, Southwest University of Science & Technology (SWUST) Mianyang, 621010, P.R. China
[2] Department of Software Engineering, Mirpur University of Science & Technology (MUST), Mirpur, Azad Jammu & Kashmir, Pakistan

**Abstract.** Over the past two decades, numerous research projects have concentrated on cognitive radio wireless sensor networks (CR-WSNs) and their benefits. To tackle the problem of energy and spectrum shortfall in CR-WSNs, this research proposes an underpinning decode-&-forward (DF) relaying technique. Using the suggested time-slot architecture (TSA), this technique harvests energy from a multi-antenna power beam (PB) and delivers source information to the target utilizing energy-constrained secondary source and relay nodes. The study considers three proposed relay selection schemes: enhanced hybrid partial relay selection (E-HPRS), conventional opportunistic relay selection (C-ORS), and leading opportunistic relay selection (L-ORS). We present evidence for the sustainability of the suggested methods by examining the outage probability (OP) and throughput (TPT) under multiple primary users (PUs). These systems leverage time switching (TS) receiver design to increase end-to-end performance while taking into account the maximum interference constraint and transceiver hardware inadequacies. In order to assess the efficacy of the proposed methods, we derive the exact and asymptotic closed-form equations for OP and TPT & develop an understanding to learn how they affect the overall performance all across the Rayleigh fading channel. The results show that OP of the L-ORS protocol is 16% better than C-ORS and 75% better than E-HPRS in terms of transmitting SNR. The OP of L-ORS is 30% better than C-ORS and 55% better than E-HPRS in terms of hardware inadequacies at the destination. The L-ORS technique outperforms C-ORS and E-HPRS in terms of TPT by 4% and 11%, respectively.

**Key words:** cognitive radio WSNs; energy harvesting; DF relaying; relay selection schemes in WSNs; hardware inadequacy in WSNs.

## 1. INTRODUCTION

Cooperative wireless communication is an effective technology in wireless sensor networks that reduces the communication gap and saves power transmission, thus making it a sustainable communication method [1]. With the use of an intermediate relay node to support transmission, use of cooperative relaying in the cooperative wireless communication has become an important application to forward source information to the destination [2]. One of the main benefits of cooperative relaying strategies is their ability to mitigate fading and attenuation, thereby improving network reliability and performance [3]. However, the selection of appropriate relays, especially in the presence of mobile nodes, remains a key challenge [4]. Technical concerns related to RF-EHNs are shown in Fig. 1. Wireless cooperative communications typically involve amplify & forward (AF) or decode & forward (DF) relaying, where a relay node harvests energy from radio frequency (RF) signals in the first phase and in the second phase utilizes that energy to transmit the source information to the destination node [5, 6]. Due to its low battery capacity, the relay node needs an additional charg-

ing system to function [5]. Research in [7] suggests that each relay divides its signals into two streams for information transmission (IT) and energy harvesting (EH). Due to the low cost, resource-constrained, and limited energy of the nodes used in WSNs, energy is a very significant resource [8, 9]. Hence, energy harvesting networks (EHNs) are essential for facilitating the information transfer through relaying, which is a sustainable technology for enhancing the energy sustainability of wireless devices with a limited lifespan. RF energy harvesting (RFEH) technique [10] has recently received research interest for its ability to convert received RF signals into electricity, making it a vital component of RF-EHNs. The Wireless Power Consortium is working to create an international standard for the RFEH technique in light of its growing uses. Several survey papers have highlighted the application scenarios of RFEH, such as sensor networks, where it can be useful and practical to combine EH and relaying in wireless cooperative communication networks [10–12].

Newer EH methods including solar, wind, thermoelectricity, harmonic distortion, electromechanical, etc., have emerged as viable alternatives to traditional EH methods [13]. Among these, RFEH has gained popularity due to its ability to transmit information and energy simultaneously, making it a promising technology for WSNs [14, 15]. In [16], the trade-off between simultaneously providing information and energy via single input

*e-mail: jianghong@swust.edu.cn

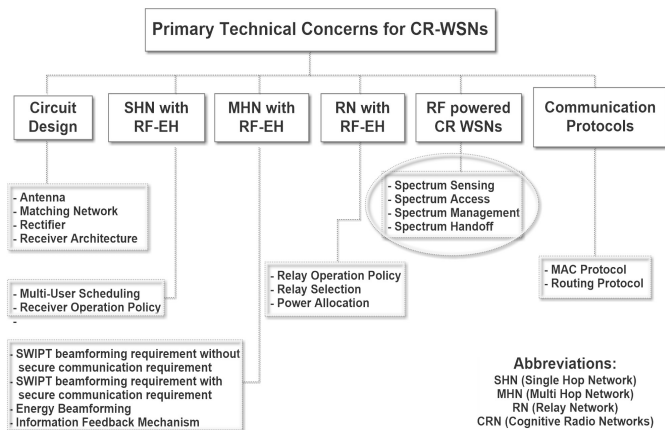M.M. Umer, H. Jiang, Q. Zhang, L. ManLu, O. Muhammad

**Fig. 1.** Technical challenges in RF-EHNs

single output (SISO) additive white Gaussian noise (AWGN) channels is examined by the authors. Building on this concept, [17] proposed the designs that are more realistically suggested and presuming that the receivers can independently decode and process the information. Multiple input multiple output (MIMO) transmission was studied by Zhang and Ho [18] using designs that divided the information decoding and EH receiver functionalities. In order to enable energy harvesting and information handling at the relay used for receiver designs based upon the aforementioned relaying approaches, two relaying protocols, i.e. time switching (TS) & power switching (PS) were established by authors in [19]. The authors in [20] examined a large network with numerous transmitter pairs and receivers that gathered energy from RF signals by using PS approach.

On the other hand, the RFEH from the source node has been the focus of numerous studies [21]. In typical communication networks, the path loss between the source and recipient is typically quite large, which weakens the RF signal and reduces the range of these systems. To address this issue and provide mobile devices with virtually unlimited battery life, researchers have presented a hybrid network with power beams (PB) positioned arbitrarily, known as Beam-assisted wireless energy transmission [22]. Also, in [23] the throughput of a distributed TDMA-based beam-assisted WSN has been explored, and furthermore, device-to-device (D2D) communication systems have looked into the beam-assisted approach [24]. Multi-hop PB-assisted relaying methods have been investigated in [25], and in order to improve system performance, special multi-hop multi-path cooperative networks with path choice strategies have been suggested in [26]. Wireless services have expanded rapidly in the past decade due to their facile connectivity anywhere and anytime leading to a scarcity of available spectrum that concerns the wireless industry [27]. One proposed solution to this problem is cognitive radio (CR) [28], that maintains the primary network quality of service (QoS) while allowing authorized PUs to share their frequency bands with unauthorized secondary users (SUs). In traditional wireless networks, SUs must periodically detect the presence of PUs to use vacant bands or relocate to other spectral gaps [29]. However, in CR-WSNs,

spectrum sensing is vital for detecting and utilizing spectrum opportunities in licensed frequency bands. Several spectrum sensing models have been introduced to improve the efficiency and accuracy of spectrum sensing in CR-WSNs, which offer various benefits, including improved spectrum utilization, reduced interference, and enhanced network capacity. The capacity of CR-WSNs to dynamically alter their transmission settings is the substantial dissimilarity between CR-WSNs, ad-hoc and standard CR-WSNs. On the other hand, the frequency bands according to licensed frequency band availability, allows for efficient spectrum utilization and improved network performance [30]. To address the limitations of spectrum sensing in CR networks, underlay CR protocols have been introduced, which enable SUs to operate continuously while sharing the spectrum with PUs & adjusting the transmit power to comply with the interference constraints. Hence, to enhance the secondary network performance, cooperative relaying protocols play a vital role. Two proactive cooperative relaying strategies, namely ORS and PRS, have been developed [31]. These methods choose the relay based on the source-relay links channel state information and seek to boost the e2e SNR. In a recent study [32], a new PRS approach has been introduced. Using the relay-destination links channel state information, this approach chooses the relay. In underlay CR networks, many relay selection methods have been discovered [33], and the performance of PRS and ORS protocols has been evaluated in terms of bit error rate (BER) and outage probability (OP) [31].

Cooperative relaying protocols can help mitigate the effects of sensor node hardware flaws including phase noise, I/Q imbalance, and amplifier nonlinearities, which can lead to a decline in performance because of cheap transceiver hardware. Björnson and Sanguinetti [34] as well as by Duy and Sanguinetti [32], have investigated the effects of hardware vulnerabilities using Nakagami-m fading channels on the dual-hop relaying networks. The latter especially examined the ergodic channel capacity and outage probability of the PRS and ORS approaches under joint inter-channel interference and as well as the hardware inadequacies. Overall, these studies highlight the importance of considering hardware inadequacies when designing and implementing cooperative relaying protocols in WSNs.

## 2. CONTRIBUTIONS

In this paper, cooperative relaying networks, underlay cognitive radio, beam assistance, hardware inadequacies, and cooperative relaying techniques are integrated to create a revolutionary cooperative spectrum sharing relaying system. The suggested schemes in this study for dual-hop DF relaying WSNs, improve both energy and spectrum efficiency, in contrast to multi-hop beam-aided relaying strategies [35–37]. We concentrate on dual-hop cooperative beam-assisted networks with unique relay selection methods. In the beginning, we suggest an E-HPRS technique that combines the traditional PRS [20] and the modified PRS [38]. The cooperative relay is selected based on the smaller value of OP using the strategy in [20], and the scheme in [38] is used otherwise. Secondly, we put forward L-ORS and C-ORS protocols to enhance the system performance. Finally,

by presenting closed-form representations of the end-to-end OP and TPT, we evaluate how well the E-HPRS, L-ORS, and C-ORS strategies perform. The derived formulations are simple to compute and can improve the system performance.

The following is a summary of this paper's substantial achievements:

- A time-slot architecture is presented in our study to enable effective energy harvesting (EH) and information transmission (IT). The suggested architecture allocates separate time-slots for IT and EH, allowing for separate slots for information transmission and specific slots for energy harvesting. Within this paradigm, we suggest three cooperative relaying approaches based on two-hop decode-and-forward (DF). Channel state information (CSI) from either the first or second hop is used in the E-HPRS approach to choosing the best relay for transmission. The C-ORS and L-ORS protocols, on the other hand, use various relay selection criteria. The L-ORS protocol chooses the relay based on the highest end-to-end signal-to-noise ratios (SNRs), while the C-ORS protocol chooses based on the biggest end-to-end (e2e) channel gain.
- For sending data from the secondary source to the secondary destination, two further relay selection techniques, C-ORS and L-ORS are presented. In C-ORS, the data is forwarded by relay having the excessive e2e channel gain. In contrast, L-ORS chooses the relay for transmission that has the highest end-to-end signal-to-noise ratio (SNR).
- We examine how interference restrictions imposed by primary users (PUs) and energy constraints imposed by the beam affect the transmission power of secondary multiple sources and relays. We also recognise how difficult it is to compare the effectiveness of the C-ORS approach to that of the E-HPRS and L-ORS programmes. This complexity results from the correlation between the first and second hop signal-to-noise ratios (SNRs), which calls for a thorough assessment of the C-ORS system.
- Considering independent & identically distributed (i.i.d.) Rayleigh fading, we have derived accurate analytical formulations and conducted asymptotic evaluation on the (OP) and (TPT) of E-HPRS, B-ORS, and C-ORS.

The rest of the paper is as follows. Section 3 provides a description of the system model. The problem formulation and presentation of different relaying selection methodologies is discussed in Section 4. Section 5 discusses the problem evaluation for the suggested scheme. Simulation & analysis is explained in Section 6, while the conclusive remarks are expressed in Section 7, i.e. Conclusions.

## 3. SYSTEM MODEL

A cooperative decode & forward (DF) multi-relaying scenario is considered for $K$ multiple sources in which the $k$-th source $S_k$, $k \in [1, 2, \ldots, K]$ communicates with the $g$-th destinations $D_g$, $g \in [1, 2, \ldots, G]$ as shown in Fig. 2. Neither any of the source nor the destination are directly connected. The information must be retransmitted through the $I$ EH-relays with $i$-th relay node $R_i$, where $i \in [1, 2, \ldots, I]$ that are deployed in each link

between the source & destination. The EH relays can obtain energy from a multi-antenna power beam $B$ where $m$-th beam $B_m$, and $m \in [1, 2, \ldots, M]$ while operating in DF mode to transmit information from source to destination. In addition, there exist $N$ interference links (PUs) where $P_n$, $n \in [1, 2, \ldots, N]$. The secondary transmitters ought to adjust their transmit power in order to strictly support dynamic spectrum access so that the interferences they cause do not impact the PUs QoS. A secondary network-deployed M-antenna power beam $(B_m)$ is required to supply power to the multiple sources and relays, which are all thought to be single-antenna, power-restricted devices. We consider the two blocks i.e. EH and IT based upon the proposed TSA (time-slot architecture). In the event that the relay receiver employs the time-switching (TS) protocol, the relay receiver contains two time-slots to perform EH and information transfer (IT) separately [15], i.e., the relay node spends some time doing this process, i.e. $(L-1)T_u$ for EH and the time $(T_u)$ for IT. So, in the absence of direct S-D link, there exists a relay in between and the information transmission in $S-R$ and $R-D$ phases is accomplished by the chosen relay using two sub-timeslots.
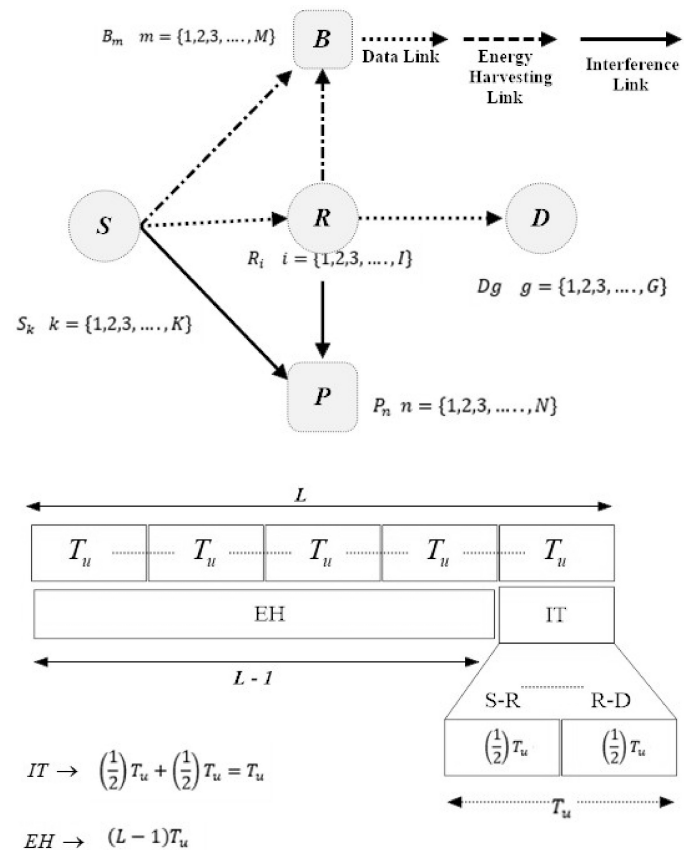


**Fig. 2.** System model (TSA)

### 3.1. Time-slot architecture

A key element of our research is the time-slot architecture (TSA), which is essential for enabling PB-assisted relay techniques in CR-WSNs while taking into account transceiver hardware inadequacies. Because time is separated into discrete slots in this design, resources may be allocated and used more ef-

*Bull. Pol. Acad. Sci. Tech. Sci.*, vol. 71, no. 5, p. e146620, 2023

3

fectively. As in our suggested framework, i.e. EH phase and IT phase, each time slot might be devoted to particular tasks or communication channels. We can efficiently control data transmission and reception, optimize resource allocation, and reduce interference inside the network by using TSA. The adaptability of the design to changing network conditions provides chances for optimization and performance improvement. We can overcome the unique difficulties given by PB-assisted relay approaches in CR-WSNs with inadequate transceiver hardware by having a thorough understanding of the TSA and its inherent advantages. The following is a detailed explanation of the proposed TSA:

The EH phase in our proposed scheme occupies many slots, but IT phase may only use a single time slot for transmission. Hence, according to the assumption, $T_u$ is employed for the whole IT phase. There are two sections in the IT block, i.e. **S-R Link** used for information transmission between source & relay and **R-D Link** used for the information transmission between relay & destination link. In sub-timeslot 1 (for **S-R Link**), the source will transmit destination data on the sub-channel allocated to $g$-th destination, and the partner $i$-th relay will receive the destination data from the source. Meanwhile, in addition to receiving the primary data, the $i$-th relay will schedule $K$ Sources to send the traffic and make use of its capabilities to receive the secondary uplink traffic. In sub-timeslot 2, the $i$-th relay forwards the data received from $k$-th source to $g$-th destination. According to this assumption, the sub-timeslot 1, i.e. $(1/2)T_u$ is employed in the **S-R Link** & the sub-timeslot 2, i.e. $(1/2)T_u$ is employed in **R-D Link**. If the $i$-th relay acts as a relay for a $g$-th destination in a sub-timeslot $(1/2)T_u$, we call $i$-th relay and $g$-th destination forms a partnership. Thus, making it $LT_u = (1/2)T_u + (1/2)T_u + (L-1)T_u$.

The channel gain between relay and destination is denoted by $\lambda S_k R_i$, $\lambda R_i D_g$ where $i, g$ and $k$ are already explained above. And, $\lambda S_k P_n$ the channel gain of interference link between $S_k$ and $P_n$, while $\lambda R_i P_n$ is the channel gain of interference link between $R_i$ and $P_n$. Similarly, the channel gain linking the $m$-th power beam antenna and the source $S_k$ and $R_i$ are $\lambda B_m S_k$ and $\lambda B_m R_i$ respectively. Suppose that Rayleigh fading occurs on every channel, leading to exponential distributions for the channel gains. Represent $\gamma_{XY}$ as the parameter of the random variable $(V)_{\lambda_{XY}}$ that is specified as $\gamma_{XY} = \dfrac{1}{E\{\lambda_{XY}\}}$ where $(XY) \in [S_k, R_i, D_g, P_n, B_m]$ & $E\{Z\}$ is an anticipated value of $VZ$. For that reason, the cumulative distribution function (C.D.F) and probability density function (P.D.F) of $V_{\lambda_{XY}}$ may be demonstrated, respectively, as:

$$CD_{\lambda_{XY}}(x) = 1 - \exp(-\gamma_{XY}x),$$
$$PD_{\lambda_{XY}}(x) = \gamma_{XY}\exp(-\gamma_{XY}x). \tag{1}$$

We may model these factors as in [39] to account for path-loss:

$$\gamma_{XY} = d_{XY}^{\beta}, \tag{2}$$

where $d_{XY}^{\beta}$ is the $X$ and $Y$ nodes link distance and $\beta$ is the path-loss exponent. Assuming that relays and interference links are

close enough to each other to form the clusters. Hence, $d_{S_k R_i} = d_{SR}, d_{S_k P_n} = d_{SP}$ and $d_{R_i P_n} = d_{RP}$ can be assumed $\forall(k, i, n)$. Similarly $\lambda_{B_m S_k}$ and $\lambda_{B_m R_i}$ can also be assumed to be $\lambda_{B_m S_k} = \lambda_{BS}$ and $\lambda_{B_m R_i} = \lambda_{BR}$ respectively $\forall(m, k, i)$. Specify $T_u$ as the total amount of time that each data transfer needs to get from source to destination.

### 3.2. Inadequacy in the hardware
For the inadequacy in the hardware, the signal received at $X \rightarrow Y$ link for the transmission is formulated as:

$$y_{XY} = \sqrt{P_X}h_{XY}(s + \iota_{XY}) + \nu_{XY} + \mu_{XY}. \tag{3}$$

The transmission power of the transmitter $X$ is $P_X$, $h_{XY}$ is the channel coefficient of the link $X \rightarrow Y$, $\mu_{XY}$ and $\iota_{XY}$ are the noise caused due to hardware inadequacy at transmitter $X$ & the receiver $Y$ subsequently, & $\nu_{XY}$ is the AWGN as Gaussian random variables with zero mean & variance $N_0$. Hence, according to the above mentioned details, SNR of $X \rightarrow Y$ link is constructed as [34, 40]:

$$\zeta = \frac{P_X \lambda_{XY}}{(\rho_X^2 + \rho_Y^2)P_X \lambda_{XY} + N_0} = \frac{P_X \lambda_{XY}}{\rho_{XY}^2 + P_X \lambda_{XY} + N_0'}, \tag{4}$$

where $\rho_X^2$ and $\rho_Y^2$ are the existing amount of the hardware inadequacies for transmitter X and receiver Y, respectively. $\rho_{XY}^2 = \rho_X^2 + \rho_Y^2$ is interpreted as an entire hardware inadequacy amount of the link $X \rightarrow Y$. Moreover, the $N_0$ is a variance of AWGN at the receiver $Y$. The inadequacy rates of information & interference linkages are presumed for convenience of the analysis and presentation as $\rho_{S_k R_i}^2 = \rho_{R_i D_g}^2$ for all $i, k$ & $g$. And, $\rho_{S_k P_n}^2 = \rho_{R_i P_n}^2 = \rho_A^2$ for all $k, i$ and $n$.

### 3.3. Energy harvesting stage
During the EH phase, beam node $B_m$ utilizes all of its antennas to provide energy to both the sources and relays. Consequently, the total harvested energy by source $S_k$ and relay $R_i$ can be stated in the following manner:

$$E_{S_k} = \eta(L-1)T_u P_{B_m} \sum_{m=1}^{M} \sum_{k=1}^{K} \lambda B_m S_k, \tag{5}$$

$$E_{R_i} = \eta(L-1)T_u P_{B_m} \sum_{m=1}^{M} \sum_{i=1}^{I} \lambda B_m R_i, \tag{6}$$

where $P_{B_m}$ is the transmit power of the beam. The energy conversion efficiency at $S_k$ and $R_i$ is denoted by $\eta$. The average transmission power that the nodes $S_k$ and $R_i$ use, can now be derived from equations (5) and (6), respectively as:

$$P_{S_k} = \frac{E_{S_k}}{(1/2)T_u} = \kappa P_{B_m} X_0^{\text{sum}}, \tag{7}$$

$$P_{R_i} = \frac{E_{R_i}}{(1/2)T_u} = \kappa P_{B_m} X_i^{\text{sum}}, \tag{8}$$

where $\kappa = 2\eta(L-1)$,

$$X_0^{\text{sum}} = \sum_{m=1}^{M} \sum_{k=1}^{K} \lambda B_m S_k \quad \text{and} \quad X_i^{\text{sum}} = \sum_{m=1}^{M} \sum_{i=1}^{I} \lambda B_m R_i.$$

4

*Bull. Pol. Acad. Sci. Tech. Sci.*, vol. 71, no. 5, p. e146620, 2023

## 3.4. Approach regarding transmission power

In underlay CR, to comply with the interference constraint, the nodes $S_k$ and $R_i$ must modify their transmission power [41], i.e.,

$$A_{S_k} \leq \frac{A_{th}}{(1+\rho_I^2)\max_{\{n=1,2,...,N\}}\lambda S_k P_n} = \frac{A_{th}}{(1+\rho_A^2)\ell_0^{\max\prime}}, \quad (9)$$

$$A_{R_i} \leq \frac{A_{th}}{(1+\rho_I^2)\max_{\{n=1,2,...,N\}}\lambda R_i P_n} = \frac{A_{th}}{(1+\rho_A^2)\ell_i^{\max\prime}}, \quad (10)$$

where $A_{th}$ represents the interference constraint threshold sought by the primary users. $P_n$, and: $\ell_0^{\max} = \max_{\{n=1,2,...,N\}}\lambda S_k P_n$ and $\ell_i^{\max} = \max_{\{n=1,2,...,N\}}\lambda R_i P_n$.

By using (7), (8), (9) and (10), the maximum transmission power of $S_k$ and $R_i$ can be constructed, subsequently as:

$$P_0 = \min\left(P_{S_k}, A_{S_k}\right) = P_{B_m}\min\left(\kappa X_0^{sum}, \frac{\omega}{\ell_o^{\max}}\right), \quad (11)$$

$$P_i = \min\left(P_{R_i}, A_{R_i}\right) = P_{B_m}\min\left(\kappa X_i^{sum}, \frac{\omega}{\ell_i^{\max}}\right). \quad (12)$$

Let $\omega = A_{th}/P_{B_m}/(1+\rho_A^2)$, and let us also define $\mu = A_{th}/P_B$, that will be taken as a constant. The instantaneous signal-to-noise ratio (SNR) generated during the 1st and 2nd hops over the relay can be summed up as follows in the existence of hardware inadequacies:

$$\zeta_{1i} = \frac{P_0 \lambda S_k R_i}{\rho_{D_g}^2 P_0 \lambda S_k R_i + N_0}$$
$$= \frac{\Delta\min(\kappa X_0^{sum}, \omega/\ell_0^{\max})\lambda S_k R_i}{\rho_{D_g}^2\Delta\min(\kappa X_0^{sum}, \omega/\ell_0^{\max})\lambda S_k R_i + 1'}, \quad (13)$$

$$\zeta_{2i} = \frac{P_i \lambda D_g R_i}{\rho_{D_g}^2 P_i \lambda D_g R_i + N_0}$$
$$= \frac{\Delta\min(\kappa X_i^{sum}, \omega/\ell_i^{\max})\lambda D_g R_i}{\rho_{D_g}^2\Delta\min(\kappa X_i^{sum}, \omega/\ell_i^{\max})\lambda D_g R_i + 1'}, \quad (14)$$

where $\Delta = \frac{P_B}{N_0}$.

By keeping DF relaying technique in mind, the end-to.end channel capacity of the $S_k \rightarrow R_i \rightarrow D_g$ path is built by:

$$C_i = \left(\frac{1}{2}\right)T_u \log_2\left(1+\min(\zeta_{1i}, \zeta_{2i})\right). \quad (15)$$

From (15), the end-to-end OP is defined by [42]:

$$OP = \Pr(C_i < C_{th}), \quad (16)$$

where the secondary network's threshold is $C_{th}$. Now, according to the mathematical expressions (16), the end-to-end TPT can be formulated as [15]:

$$TPT = (T_u)C_{th}(1-OP). \quad (17)$$

## 4. RELAY SELECTION METHODOLOGIES

### 4.1. Proposed enhanced-HPRS (E-HPRS) in line with hybrid PRS (H-PRS)

According to the traditional partial relay selection (PRS) protocol [43], the data is forwarded to the destination by the relay that offers the highest channel gain on the very first hop. In terms of mathematics, we express:

$$R_{a_1}: \lambda S_k R_{a_1} = \max_{i=1,2,...,I}\lambda S_k R_i, \quad (18)$$

where $R_{a_1}$ is the chosen relay with $a_1 \in \{1,2,...,I\}$. The following method is used to choose the best relay for the PRS protocol suggested in [38].

$$R_{a_2}: \lambda R_{a_2} D_g = \max_{i=1,2,...,I}\lambda R_i D_g, \quad (19)$$

where $a_2 \in \{1,2,...,I\}$. Now combining (15), (16), (18) and (19), the end-to-end OP of the PRS methodologies in [43] and [38] can respectively be defined as follows:

$$OP_{PRS1} = \Pr(C_{a_1} < C_{th})$$
$$= \Pr\left(\left(\frac{1}{2}\right)T_u \log_2(1+\min(\zeta_{1_{a_1}}, \zeta_{2_{a_2}})) < C_{th}\right), \quad (20)$$

$$OP_{PRS2} = \Pr(C_{a_2} < C_{th})$$
$$= \Pr\left(\left(\frac{1}{2}\right)T_u \log_2(1+\min(\zeta_{1_{a_1}}, \zeta_{2_{a_2}})) < C_{th}\right). \quad (21)$$

In our proposed scheme, we use $(1/2)T_u$ instead of $((1-\alpha)/2)T_u$ (used in HPRS (hybrid partial relay selection) by neglecting $\alpha$. As for the larger $L$ values, the smaller $\alpha$ seems meaningless in the model. Thus, ignoring the parameter $\alpha$, further simplifies our model. Hence, according to the proposed model, if $OP_{PRS1} \leq OP_{PRS2}$, then the best relay is picked by using (18) and if $OP_{PRS1} > OP_{PRS2}$, the selection procedure described in (19) is employed to choose the best relay for the collaboration. Hence, as a conclusion, the E-HPRS protocol outage performance is represented as:

$$OP_{E\text{-}HPRS} = \min(OP_{PRS1}, OP_{PRS2}). \quad (22)$$

So, the end-to-end throughput by using the proposed protocol i.e. E-HPRS can be obtained by:

$$TPT_{E\text{-}HPRS} = (T_u)C_{th}(1-OP_{E\text{-}HPRS}). \quad (23)$$

### 4.2. Leading ORS (L-ORS)

The best relay in the L-ORS is picked in order to increase the end-to-end SNR, i.e.

$$R_b: \min(\zeta_{1b}, \zeta_{2b}) = \max_{i=1,2,...,I}(\min(\zeta_{1i}, \zeta_{2i})), \quad (24)$$

where $b \in \{1,2,...,I\}$.

*Bull. Pol. Acad. Sci. Tech. Sci.*, vol. 71, no. 5, p. e146620, 2023

5

M.M. Umer, H. Jiang, Q. Zhang, L. ManLu, O. Muhammad

Now, the end-to-end TPT performance of this scheme is given, respectively, by:

$$\text{OP}_{\text{L-ORS}} = \text{P}_\text{r}\left(\left(\frac{1}{2}\right)T_u \log_2(1+\min(\zeta_{1b},\zeta_{2b})) < C_{th}\right), \quad (25)$$

$$\text{TPT}_{\text{L-ORS}} = (T_u)C_{th}(1-\text{OP}_{\text{L-ORS}}). \quad (26)$$

### 4.3. Conventional ORS (C-ORS)

As proposed in many papers such as [32, 44–46], in order to boost the information link end-to-end SNR, the suitable relay is chosen:

$$\text{R}_\text{c}: \ \min(\lambda S_k R_c, \lambda R_c D_g) = \min_{1,2,\dots,I}(\min(\lambda S_k R_i, \lambda R_i D_g)), \quad (27)$$

where $c \in \{1,2,\dots,I\}$. Then, the end-to-end OP and TPT of the C-ORS protocol is computed, respectively, as:

$$\text{OP}_{\text{C-ORS}} = \text{P}_\text{r}\left(\left(\frac{1}{2}\right)T_u \log_2(1+\min(\zeta_{1c},\zeta_{2c})) < C_{th}\right), \quad (28)$$

$$\text{TPT}_{\text{C-ORS}} = (T_u)C_{th}(1-\text{OP}_{\text{C-ORS}}). \quad (29)$$

## 5. PERFORMANCE EVALUATION

### 5.1. Outage probability

Generally, the end-to-end OP of the protocol $U, U \in \{\text{E-HPRS}, \text{L-ORS}, \text{C-ORS}\}$, is possible to describe in the following way:

$$\begin{aligned}\text{OP}_\text{U} &= \text{P}_\text{r}(\min(\zeta_{1l},\zeta_{2l}) < \theta) \\ &= 1 - \text{P}_\text{r}(\min(\zeta_{1l},\zeta_{2l}) \geq \theta) \\ &= 1 - \text{P}_\text{r}(\zeta_{1l} \geq \theta, \ \zeta_{2l} \geq \theta),\end{aligned} \quad (30)$$

where $l \in \{a_1, a_2, b, c\}$ and $\theta = 2^{\frac{2C_{th}}{T_u}} - 1$. In addition, now, substituting (13) and (14) into (30), which yields:

$$\begin{aligned}\text{OP}_\text{U} = 1 - \text{P}_\text{r}&\left((1-\rho_{D_g}^2 \theta)\Delta\min\left(\kappa X_0^{\text{sum}}, \frac{\omega}{l_0^{\max}}\right)\lambda S_k R_l \geq \theta,\right.\\ &\left.(1-\rho_{D_g}^2)\Delta\min\left(\kappa X_l^{\text{sum}}, \frac{\omega}{l_l^{\max}}\right)\lambda R_l D_g \geq \theta\right).\end{aligned} \quad (31)$$

It is obvious from equation (31) that $\text{OP}_\text{U} = 1$, if $1-\rho_{D_g}^2 \theta \leq 0$. Going to assume that $1-\rho_{D_g}^2 \theta > 0$, the aforementioned equation may be written in the following format:

$$\begin{aligned}\text{OP}_\text{U} = 1 - \text{P}_\text{r}&\left(\min\left(\kappa X_0^{\text{sum}}, \frac{\omega}{l_0^{\max}}\right)\lambda S_k R_l \geq \frac{\rho}{\Delta},\right.\\ &\left.\min\left(\kappa X_l^{\text{sum}}, \frac{\omega}{l_l^{\max}}\right)\lambda R_l D_g \geq \frac{\rho}{\Delta}\right),\end{aligned} \quad (32)$$

where $\rho = \theta/(1-\rho_{D_g}^2 \theta)$.

**Lemma 1.** As $1-\rho_{D_g}^2 \theta > 0$, then the closed-form expression of $\text{OP}_{\text{PRS1}}$ and $\text{OP}_{\text{PRS2}}$ are as follows:

$$\begin{aligned}\text{OP}_{\text{PRS1}} = 1 - &\left[\sum_{t=0}^{M-1}\sum_{i=0}^{I-1}(-1)^i\frac{2C_{I-1}^i I}{t!}(m+1)^{\frac{t-1}{2}}\left(\frac{\gamma_{B_m S_k}\gamma_{S_k R_i}\rho}{\kappa\Delta}\right)^{\frac{t+1}{2}}M_{1-t}\left(2\sqrt{\frac{(i+1)\gamma_{B_m S_k}\gamma_{S_k R_i}\rho}{\kappa\Delta}}\right)\right.\\ &-\sum_{t=0}^{M-1}\sum_{n=1}^{N}\sum_{i=0}^{I-1}(-1)^{n+i+1}C_{I-1}^i C_N^n\frac{2I\gamma_{S_k R_i}}{t!}\left(\frac{\rho}{n\gamma_{S_k P_n}\omega\Delta+(i+1)\gamma_{S_k R_i}\rho}\right)^{\frac{1-t}{2}}\left(\frac{\gamma_{B_m S_k}\rho}{\kappa\Delta}\right)^{\frac{t+1}{2}}\\ &\times M_{1-t}\left(2\sqrt{\frac{\gamma_{B_m S_k}}{\kappa\Delta}(n\gamma_{S_k P_n}\omega\Delta+(i+1)\gamma_{S_k R_i}\rho)}\right)\times\left[\sum_{t=0}^{M-1}\frac{2}{t!}\left(\frac{\gamma_{B_m R_i}\gamma_{R_i D_g}\rho}{\kappa\Delta}\right)^{\frac{t+1}{2}}M_{1-t}\left(2\sqrt{\frac{\gamma_{B_m R_i}\gamma_{R_i D_g}\rho}{\kappa\Delta}}\right)\right.\\ &-\left.\left.\sum_{t=0}^{M-1}\sum_{n=1}^{N}(-1)^{n+1}c_N^n\frac{2\gamma_{R_i D_g}}{t!}\left(\frac{\rho}{n\gamma_{R_i P_n}\omega\Delta+\gamma_{R_i D_g}\rho}\right)^{\frac{1-t}{2}}\left(\frac{\gamma_{B_m R_i}\rho}{\kappa\Delta}\right)^{\frac{t+1}{2}}\times M_{1-t}\left(2\sqrt{\frac{\gamma_{B_m R_i}}{\kappa\Delta}(n\gamma_{R_i P_n}\omega\Delta+\gamma_{R_i D_g}\rho)}\right)\right]\right], \quad (33)\end{aligned}$$

$$\begin{aligned}\text{OP}_{\text{PRS2}} = 1 - &\left[\sum_{t=0}^{M-1}\sum_{i=0}^{I-1}(-1)^i\frac{2C_{I-1}^i I}{t!}(m+1)^{\frac{t-1}{2}}\left(\frac{\gamma_{B_m R_i}\gamma_{R_i D_g}\rho}{\kappa\Delta}\right)^{\frac{t+1}{2}}M_{1-t}\left(2\sqrt{\frac{(i+1)\gamma_{B_m R_i}\gamma_{R_i D_g}\rho}{\kappa\Delta}}\right)\right.\\ &-\sum_{t=0}^{M-1}\sum_{n=1}^{N}\sum_{i=0}^{I-1}(-1)^{n+i+1}C_{I-1}^i C_N^n\frac{2I\gamma_{R_i D_g}}{t!}\left(\frac{\rho}{n\gamma_{R_i P_n}\omega\Delta+(i+1)\gamma_{R_i D_g}\rho}\right)^{\frac{1-t}{2}}\left(\frac{\gamma_{B_m R_i}\rho}{\kappa\Delta}\right)^{\frac{t+1}{2}}\\ &\times M_{1-t}\left(2\sqrt{\frac{\gamma_{B_m R_i}}{\kappa\Delta}(n\gamma_{R_i P_n}\omega\Delta+(i+1)\gamma_{R_i D_g}\rho)}\right)\times\left[\sum_{t=0}^{M-1}\frac{2}{t!}\left(\frac{\gamma_{B_m S_k}\gamma_{S_k R_i}\rho}{\kappa\Delta}\right)^{\frac{t+1}{2}}M_{1-t}\left(2\sqrt{\frac{\gamma_{B_m S_k}\gamma_{S_k R_i}\rho}{\kappa\Delta}}\right)\right.\\ &-\left.\left.\sum_{t=0}^{M-1}\sum_{n=1}^{N}(-1)^{n+1}c_N^n\frac{2\gamma_{S_k R_i}}{t!}\left(\frac{\rho}{n\gamma_{S_k P_n}\omega\Delta+\gamma_{S_k R_i}\rho}\right)^{\frac{1-t}{2}}\left(\frac{\gamma_{B_m S_k}\rho}{\kappa\Delta}\right)^{\frac{t+1}{2}}\times M_{1-t}\left(2\sqrt{\frac{\gamma_{B_m S_k}}{\kappa\Delta}(n\gamma_{S_k P_n}\omega\Delta+\gamma_{S_k R_i}\rho)}\right)\right]\right], \quad (34)\end{aligned}$$

6

*Bull. Pol. Acad. Sci. Tech. Sci.*, vol. 71, no. 5, p. e146620, 2023

**Lemma 2.** As $1 - \rho_{D_g}^2 \theta > 0$, then the closed-form expression of $\text{OP}_{\text{L-ORS}}$ can be given as:

$$
\begin{aligned}
\text{OP}_{\text{L-ORS}} = 1 + \sum_{t=0}^{M-1} \sum_{i=1}^{I} (-1)^i \frac{2C_I^i}{t!} \left( \frac{i\gamma_{B_m S_k} \gamma_{S_k R_i} \rho}{\kappa\Delta} \right)^{\frac{t+1}{2}} M_{t-1}\left( 2\sqrt{\frac{i\gamma_{B_m S_k} \gamma_{S_k R_i} \rho}{\kappa\Delta}} \right) \\
\times \Bigg[ \sum_{t=0}^{M-1} \frac{2}{t!} \left( \frac{\gamma_{B_m R_i} \gamma_{R_i D_g} \rho}{\kappa\Delta} \right)^{\frac{t+1}{2}} M_{1-t}\left( 2\sqrt{\frac{\gamma_{B_m R_i} \gamma_{R_i D_g} \rho}{\kappa\Delta}} \right) \\
- \sum_{t=0}^{M-1} \sum_{n=1}^{N} (-1)^{n+1} C_N^n \frac{2\gamma_{R_i D_g}}{t!} \left( \frac{\rho}{n\gamma_{R_i P_n} \omega\Delta + \gamma_{R_i D_g}\rho} \right)^{\frac{1-t}{2}} \left( \frac{\gamma_{B_m R_i}}{\kappa\Delta} \right)^{\frac{t+1}{2}} M_{1-t}\left( 2\sqrt{\frac{\gamma_{B_m R_i}}{\kappa\Delta}(n\gamma_{R_i P_n}\omega\Delta + \gamma_{R_i D_g}\rho)} \right) \Bigg]^i \\
+ \sum_{t=0}^{M-1} \sum_{n=1}^{N} \sum_{i=1}^{I} (-1)^{m+n} \frac{2C_N^n C_I^i}{t!} \left( \frac{i\gamma_{B_m S_k} \gamma_{S_k R_i} \rho}{\kappa\Delta} \right)^{\frac{t+1}{2}} \left( 1 + \frac{n\gamma_{S_k P_n} \omega\Delta}{i\gamma_{S_k R_i}\rho} \right)^{\frac{t-1}{2}} M_{t-1}\left( 2\sqrt{\frac{\gamma_{B_m S_k}}{\kappa\Delta}(n\gamma_{S_k P_n}\omega\Delta + i\gamma_{S_k R_i}\rho)} \right) \\
\times \Bigg[ \sum_{t=0}^{M-1} \frac{2}{t!} \left( \frac{\gamma_{B_m R_i} \gamma_{R_i D_g} \rho}{\kappa\Delta} \right)^{\frac{t+1}{2}} M_{1-t}\left( 2\sqrt{\frac{\gamma_{B_m R_i} \gamma_{R_i D_g} \rho}{\kappa\Delta}} \right) - \sum_{t=0}^{M-1} \sum_{n=1}^{N} (-1)^{n+1} \\
C_N^n \frac{2\gamma_{R_i D_g}}{t!} \left( \frac{\rho}{n\gamma_{R_i P_n} \omega\Delta + \gamma_{R_i D_g}\rho} \right)^{\frac{1-t}{2}} \left( \frac{\gamma_{B_m R_i}\rho}{\kappa\Delta} \right)^{\frac{t+1}{2}} M_{1-t}\left( 2\sqrt{\frac{\gamma_{B_m R_i}}{\kappa\Delta}(n\gamma_{R_i P_n}\omega\Delta + \gamma_{R_i D_g}\rho)} \right) \Bigg]^i .
\end{aligned}
\tag{35}
$$

**Lemma 3.** As $1 - \rho_{D_g}^2 \theta > 0$, then the closed-form expression of $\text{OP}_{\text{C-ORS}}$ can be given as:

$$
\begin{aligned}
\text{OP}_{\text{C-ORS}} = 1 - \sum_{i=0}^{I-1} \sum_{t=0}^{M-1} \sum_{n=0}^{N} \sum_{\delta=0}^{M-1} \sum_{q=0}^{N} (-1)^{i+n+q} C_{I-1}^i \frac{C_N^n C_N^q}{t!\delta!} \left( \frac{\gamma_{B_m S_k}}{\kappa} \right)^t \left( \frac{\gamma_{B_m R_i}}{\kappa} \right)^\delta \frac{I\gamma_{R_i D_g}}{\gamma_{R_i D_g} + i\Omega} \\
\times \int_0^{+\infty} \int_0^{z_2} \left( \frac{\gamma_{B_m S_k}}{\kappa} z_1^t - n\gamma_{S_k P_n}\omega z_1^{t-2} - t z_1^{t-1} \right) \left( \frac{\gamma_{B_m R_i}}{\kappa} z_2^\delta - q\gamma_{R_i P_n}\omega z_2^{\delta-2} - \delta z_2^{\delta-1} \right) \times \exp\left( -\frac{\gamma_{S_k R_i}\rho}{\Delta} \frac{1}{z_1} \right) \\
\times \exp\left( -\frac{(\gamma_{R_i D_g} + i\Omega)\rho}{\Delta} \frac{1}{z_2} \right) \exp\left( -\frac{\gamma_{B_m S_k}}{\kappa} z_1 - \frac{n\gamma_{S_k P_n}\omega}{z_1} \right) \exp\left( -\frac{\gamma_{B_m R_i}}{\kappa} z_2 - \frac{q\gamma_{R_i P_n}\omega}{z_2} \right) dz_1 dz_2 \\
- \sum_{t=0}^{M-1} \sum_{n=0}^{N} \sum_{\delta=0}^{M-1} \sum_{q=0}^{N} (-1)^{i+n+q} C_{I-1}^i \frac{C_N^n C_N^q}{t!\delta!} \left( \frac{\gamma_{B_m S_k}}{\kappa} \right)^t \left( \frac{\gamma_{B_m R_i}}{\kappa} \right)^\delta \frac{\frac{i}{i+1} I\gamma_{S_k R_i}}{\gamma_{R_i D_g} + i\Omega} \\
\times \int_0^{+\infty} \int_0^{z_2} \left( \frac{\gamma_{B_m S_k}}{\kappa} z_1^t - n\gamma_{S_k P_n}\omega z_1^{t-2} - t z_1^{t-1} \right) \left( \frac{\gamma_{B_m R_i}}{\kappa} z_2^\delta - q\gamma_{R_i P_n}\omega z_2^{\delta-2} - \delta z_2^{\delta-1} \right) \times \exp\left( -\frac{(i+1)\Omega\rho}{\Delta} \frac{1}{z_1} \right) \\
\exp\left( -\frac{\gamma_{B_m S_k}}{\kappa} z_1 - \frac{n\gamma_{S_k P_n}\omega}{z_1} \right) \exp\left( -\frac{\gamma_{B_m S_k}}{\kappa} z_2 - \frac{q\gamma_{R_i P_n}\omega}{z_2} \right) dz_1 dz_2 \sum_{t=0}^{M-1} \sum_{n=0}^{N} \sum_{\delta=0}^{M-1} \sum_{q=0}^{N} (-1)^{i+n+q} C_{I-1}^i \frac{C_N^n C_N^q}{t!\delta!} \left( \frac{\gamma_{B_m S_k}}{\kappa} \right)^t \\
\left( \frac{\gamma_{B_m R_i}}{\kappa} \right)^\delta \frac{I\gamma_{S_k R_i}}{\gamma_{S_k R_i} + i\Omega} \times \int_0^{+\infty} \int_0^{z_2} \left( \frac{\gamma_{B_m S_k}}{\kappa} z_1^t - n\gamma_{S_k P_n}\omega z_1^{t-2} - t z_1^{t-1} \right) \left( \frac{\gamma_{B_m R_i}}{\kappa} z_2^\delta - q\gamma_{R_i P_n}\omega z_2^{\delta-2} - \delta z_2^{\delta-1} \right) \\
\times \exp\left( -\frac{\gamma_{R_i D_g}\rho}{\Delta} \frac{1}{z_2} \right) \exp\left( -\frac{(\gamma_{S_k R_i} + i\Omega)\rho}{\Delta} \frac{1}{z_1} \right) \exp\left( -\frac{\gamma_{B_m S_k}}{\kappa} z_1 - \frac{n\gamma_{S_k P_n}\omega}{z_1} \right) \\
\times \exp\left( -\frac{\gamma_{B_m S_k}}{\kappa} z_2 - \frac{q\gamma_{R_i P_n}\omega}{z_2} \right) dz_1 dz_2 \sum_{t=0}^{M-1} \sum_{n=0}^{N} \sum_{\delta=0}^{M-1} \sum_{q=0}^{N} (-1)^{i+n+q} C_{I-1}^i \frac{C_N^n C_N^q}{t!\delta!} \left( \frac{\gamma_{B_m S_k}}{\kappa} \right)^t \left( \frac{\gamma_{B_m R_i}}{\kappa} \right)^\delta \frac{I\gamma_{S_k R_i}}{\gamma_{S_k R_i} + i\Omega} \\
\times \int_0^{+\infty} \int_0^{z_2} \left( \frac{\gamma_{B_m S_k}}{\kappa} z_1^t - n\gamma_{S_k P_n}\omega z_1^{t-2} - t z_1^{t-1} \right) \left( \frac{\gamma_{B_m R_i}}{\kappa} z_2^\delta - q\gamma_{R_i P_n}\omega z_2^{\delta-2} - \delta z_2^{\delta-1} \right) \\
\times \exp\left( -\frac{(i+1)\Omega\rho}{\Delta} \frac{1}{z_1} \right) \exp\left( -\frac{\gamma_{B_m S_k}}{\kappa} z_1 - \frac{n\gamma_{S_k P_n}\omega}{z_1} \right) \exp\left( -\frac{\gamma_{B_m S_k}}{\kappa} z_2 - \frac{q\gamma_{R_i P_n}\omega}{z_2} \right) dz_1 dz_2 .
\end{aligned}
\tag{36}
$$

*Bull. Pol. Acad. Sci. Tech. Sci.*, vol. 71, no. 5, p. e146620, 2023

7

As mentioned in equation (22), we have $\text{OP}_{\text{E-HPRS}} = \min(\text{OP}_{\text{PRS1}}, \text{OP}_{\text{PRS2}})$. The E-HPRS protocol can also be implemented in the manner described below. We initially suppose that the $S_k$ source and the $D_g$ destination are capable of understanding the data link statistical specifics, i.e. ($\gamma_{S_k R_i}$, $\gamma_{R_i D_g}$), the interference links, i.e. ($\gamma_{S_k P_n}$, $\gamma_{R_i P_n}$) and the EH links, i.e. ($\gamma_{B_m S_k}$, $\gamma_{B_m R_i}$). When the instantaneous CSI is averaged [47,48], the statistical channel state information can be easily derived in practice and made sure that all nodes via system messages are informed. The source and destination nodes then can calculate $\text{OP}_{\text{PRS1}}$ and $\text{OP}_{\text{PRS2}}$ by using the exact closed form expressions of end-to-end outage probability for E-HPRS protocol. And at last, the source/destination may decide to use the procedure outlined in [43] or in [38] for S-D data transmission by contrasting $\text{OP}_{\text{PRS1}}$ and $\text{OP}_{\text{PRS2}}$.

## 5.2. Throughput
By inserting the equations for the OP into the E-HPRS, C-ORS, and B-ORS protocols, it is feasible to figure out the throughput (TPT) of those protocols by using (17).

## 6. SIMULATION AND ANALYSIS
The effectiveness of three suggested systems for EH DF cooperative relay selection is shown in this section through a series of theoretical calculations that additionally take interference restrictions from various PUs into account. Monte Carlo simulations are used to validate the theoretical equations. The nodes $S_k$ in the simulation environment are situated around the origin in Cartesian coordinates. The simulation parameters are shown in Table 1.

**Table 1**
Simulation parameters

| | |
|---|---|
| $(x_R, 0)$ | Coordinates of relay $R_i$ |
| $(x_D, 0)$ | Coordinates of destination $D_g$ |
| $(0.5, 0.5)$ | Coordinates of beam $B_m$ |
| $(x_p, y_p)$ | Coordinates of primary users $P_n$ |
| $\mu = 0.25$ | The ratio between $I_{th}$ and $P_B$ |
| $\beta = 3$ | The path-loss exponent |
| $T_u = 1$ | The time taken for each transmission of data |
| $N = 2$ | No. of primary users |
| $L = 10$ | No. of time-slots |
| $\eta = 1$ | Energy conversion efficiency |
| $M = 2$ | The number of antennas at the power beam |

## 6.1. OP of PRS protocols as a function of $x_R$
In Fig. 3, we show the outage probability (OP) as a function of $x_R$ for the proposed EH-PRS protocol, the modified PRS protocol, and the traditional PRS protocol [33] (denoted by PRS1 and PRS2, respectively). Next, we can observe that PRS1 has a greater OP than PRS2 since $x_R$ is small (the relays are near

the source but they are far from the destination). Yet, PRS1 outperforms PRS2 since $x_R$ is sufficient enough. As we can see, the operation of E-HPRS is identical to the operation of PRS1, because the relays are close to the destinations and to the operation of PRS2 when the relays are closer to a number of sources. Moreover, the OP values of PRS1 and PRS2 exist at a value of $x_R$ (designated $x_R^*$). In fact, we may determine the value of $x_R^*$ by resolving the equation $\text{OP}_{\text{PRS1}} = \text{OP}_{\text{PRS2}}$ (using (33) and (34)). Finally, it can be seen from Fig. 3 that improving the transmit SNR ($\Delta$), improves the outage performance of PRS1, PRS2, and E-HPRS.
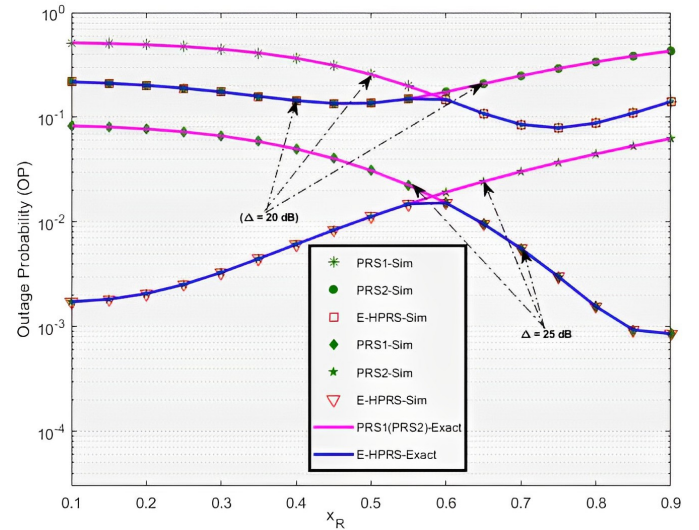


**Fig. 3.** Outage probability of the PRS protocols as a function of $x_R$

## 6.2. $x_R^*$ as a function of $x_p$
In Fig. 4, the values of $x_R^*$ are shown for different positions ($y_p$) of primary users $P_n$. The equation $\text{OP}_{\text{PRS1}} = \text{OP}_{\text{PRS1}}$ is solved to obtain $x_R^*$, which is a reference distance between sources and relays used in E-HPRS. This distance determines whether to use PRS1 or PRS2 to transmit source data to the destination.
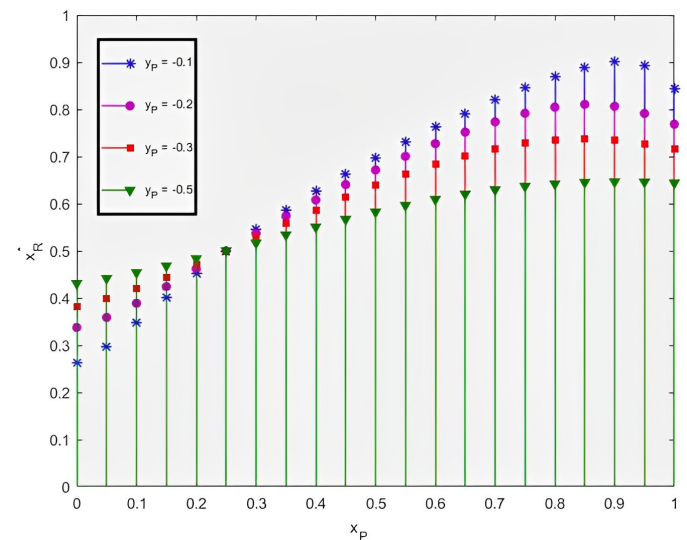


**Fig. 4.** $x_R^*$ as a function of $x_P$

8

*Bull. Pol. Acad. Sci. Tech. Sci.*, vol. 71, no. 5, p. e146620, 2023

If $x_R < x_R^*$, PRS2 is used, while if $x_R > x_R^*$, the system employs PRS1. According to Fig. 4, the position of primary users significantly affects $x_R^*$. When primary users are close to the sources ($x_P$ is small), the value of $x_R^*$ is low, and vice versa.

### 6.3. OP as a function of $\Delta$

Using different choices of $C_{th}$, the outage performance of E-HPRS, L-ORS, and C-ORS is analyzed in Fig. 5. OP of L-ORS is lowest, while OP of E-HPRS is highest, as can be seen. The OP of L-ORS and C-ORS swiftly drops as $\Delta$ increases at high transmit SNR. This is because, when compared to E-HPRS, the bigger diversity gains are achieved by L-ORS and C-ORS.
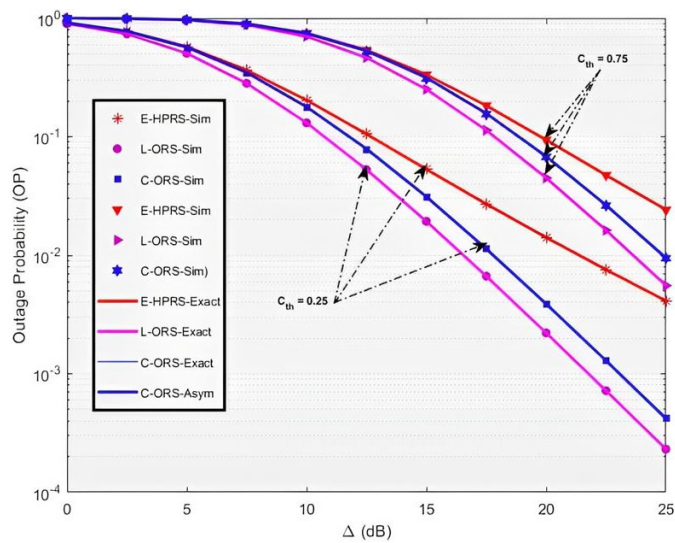


**Fig. 5.** Outage probability as a function of $\Delta$ in dB

### 6.4. OP as a function of $x_R$

According to the proposed scheme, we exhibit that the relays are placed on the x-axis ($x_R$) and OP to be its function. It is carried out to assess how distances impact the efficiency of the proposed schemes in the event of an outage. Figure 6 shows
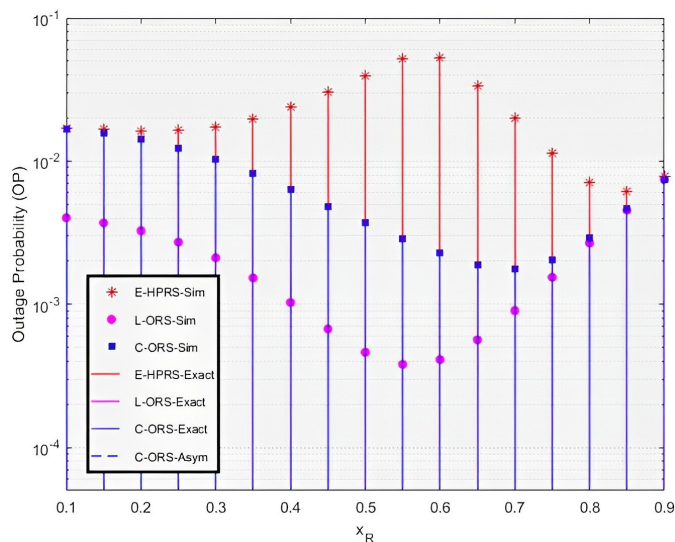


**Fig. 6.** Outage probability as a function of $x_R$

that there is a relay placement that is optimum and at which the L-ORS and C-ORS have the minimum OP values. It can be concluded that when the relays are closer to the source, the performance of E-HPRS is comparable to C-ORS. Another intriguing finding is that when the relays are nearer to the destinations, the OP value of E-HPRS reaches that of L-ORS and C-ORS. It is explained by the fact that, when the relays are nearest to the destinations, the operation of all methodologies is largely dependent on the S-R link; as a result, E-HPRS can be roughly contrasted to L-ORS and C-ORS. When the relays are placed between the source and the destination, E-HPRS performs less effectively as compared to L-ORS and C-ORS. For instance, the OP of E-HPRS is maximum when $x_R$ is close to 0.6.

### 6.5. OP as a function of $\rho_{D_g}^2$

In Fig. 7, we examine how the hardware inadequacy level ($\rho_{D_g}^2$) affects the functionality of the E-HPRS, L-ORS, and C-ORS. It is apparent that as $\rho_{D_g}^2$ increases, the OP values rise quickly. Furthermore, Fig. 7 demonstrates that when $\rho_{D_g}^2$ is greater than 0.55, all of the proposed schemes are always in the outage. According to Section 3, if $\rho_{D_g}^2 \geq 0.55$, then $1 - \rho_{D_g}^2 \theta < 0$ and hence $OP_{E\text{-HPRS}} = OP_{L\text{-ORS}} = OP_{C\text{-ORS}} = 1$.
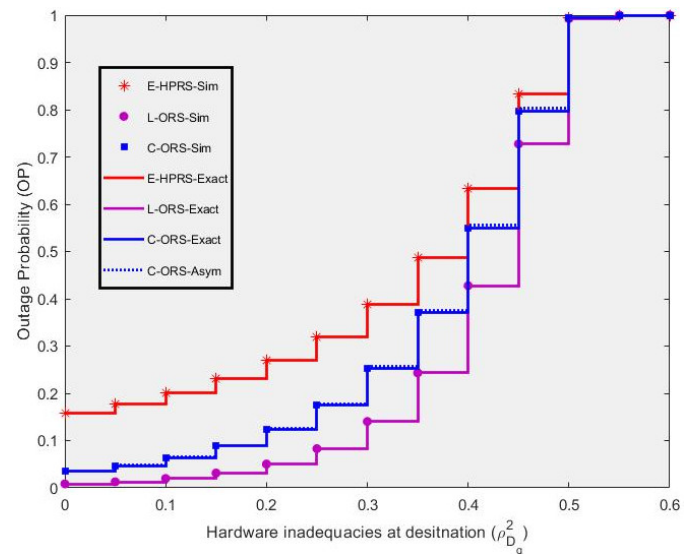


**Fig. 7.** Outage probability as a function of $\rho_{D_g}^2$

### 6.6. TPT as a function of $I$

Figure 8 depicts the relationship between end-to-end TPT and the number of relays ($I$). As expected, raising the $I$ value by keeping $T_u$ under consideration can improve the throughput of E-HPRS, L-ORS, and C-ORS. Likewise, it is clear that giving the values effectively can enhance the performance of the protocols under consideration. The simulation outcomes are unmistakably in perfect accord with the theoretical values that we have established, and the minor discrepancy between the exact and asymptotic results demonstrates the resolution of our theoretical foundations.
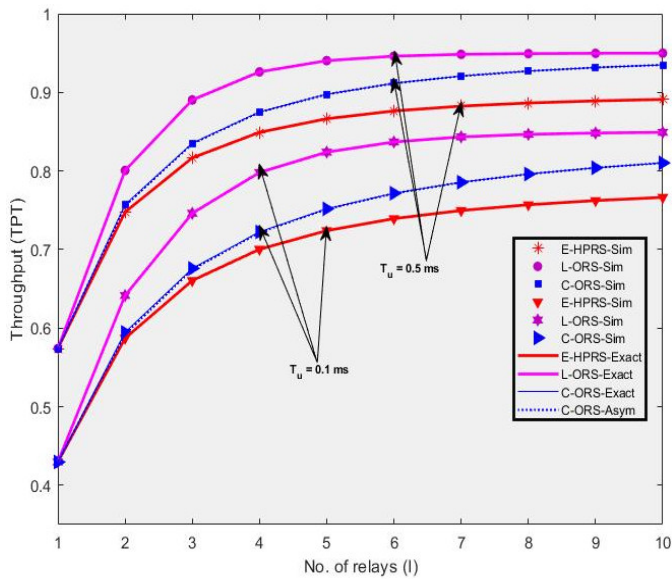
*Bull. Pol. Acad. Sci. Tech. Sci.*, vol. 71, no. 5, p. e146620, 2023

9

M.M. Umer, H. Jiang, Q. Zhang, L. ManLu, O. Muhammad

**Fig. 8.** Throughput as a function of *I*

## 7. CONCLUSION

In this study, we sought to improve the performance of cooperative relaying wireless sensor networks with beam-assisted underlay cognitive radio (CR) in the face of hardware inadequacies and interference constraints. We put forward three 3 protocols that make use of multiple antenna beams to do dual-hop decode-and-forward (DF) relaying operations by using the proposed time-slot architecture (TSA). By analyzing the outage probability (OP) and throughput (TPT) under Rayleigh fading channels and multiple primary users (PUs), we provided evidence supporting the viability of the suggested schemes. Specifically, the numerical results showed that the L-ORS protocol outperformed the C-ORS and E-HPRS protocols in terms of performance gains. We also found that system performance may be further enhanced by enhancing the EH ratio, increasing the No. of relays, and more importantly, carefully situating the relays. Overall, our study provides insights into the design of beam-assisted underlay CR systems in wireless sensor networks and demonstrates the potential for improved performance through innovative relaying protocols. The results show that OP of the L-ORS protocol is 16% better than C-ORS and 75% better than E-HPRS in terms of transmit SNR. The OP of L-ORS is 30% better than C-ORS and 55% better than E-HPRS in terms of hardware inadequacies at the destination. The L-ORS technique outperforms C-ORS and E-HPRS in terms of TPT by 4% and 11%, respectively.

## ACKNOWLEDGEMENTS

## REFERENCES

[1] W. Hu, J. Si, and H. Li, "Security-reliability tradeoff analysis in multisource multirelay cooperative networks with multiple cochannel interferers," *Wirel. Commun. Mob. Comput.*, vol. 2018, p. 2379427, 2018.

[2] S. Parkouk, M. Torabi, and S. Shokrollahi, "Secrecy performance analysis of amplify-and-forward relay cooperative networks with simultaneous wireless information and power transfer," *Comput. Commun.*, vol. 193, pp. 365–377, 2022.

[3] I. Muhammad, H. Alves, O.A. Lopez, and M. Latva-aho, "Secure rate control and statistical qos provisioning for cloud-based iot networks," *Secur. Commun. Netw.*, vol. 2021, pp. 1–19, 2021.

[4] M. Asam, Z. Haider, T. Jamal, K. Ghuman, and A. Ajaz, "Novel relay selection protocol for cooperative networks," *arXiv preprint arXiv:1911.07764*, 2019.

[5] A.A. Nasir, X. Zhou, S. Durrani, and R.A. Kennedy, "Wireless-powered relays in cooperative communications: Time-switching relaying protocols and throughput analysis," *IEEE Trans. Commun.*, vol. 63, no. 5, pp. 1607–1622, 2015.

[6] S.D. Roy, S. Kundu, A. Kumar, and S. Sharma, "Secrecy outage probability with destination assisted jamming in presence of an untrusted relay," in *2016 IEEE Annual India Conference (INDICON)*. IEEE, 2016, pp. 1–5.

[7] H.H. Chen, Y. Li, Y. Jiang, Y. Ma, and B. Vucetic, "Distributed power splitting for swipt in relay interference channels using game theory," *IEEE Trans. Wirel. Commun.*, vol. 14, no. 1, pp. 410–420, 2014.

[8] H. Lin, D. Bai, D. Gao, and Y. Liu, "Maximum data collection rate routing protocol based on topology control for rechargeable wireless sensor networks," *Sensors*, vol. 16, no. 8, p. 1201, 2016.

[9] Z. Wang, P. Zeng, M. Zhou, D. Li, and J. Wang, "Cluster-based maximum consensus time synchronization for industrial wireless sensor networks," *Sensors*, vol. 17, no. 1, p. 141, 2017.

[10] H.J. Visser and R.J. Vullers, "Rf energy harvesting and transport for wireless sensor network applications: Principles and requirements," *Proc. IEEE*, vol. 101, no. 6, pp. 1410–1423, 2013.

[11] S. Gujral, S. Sarma, and S. Banerjee, "Transmit power minimization in bidirectional tag-to-device communications for iot," in *2021 International Conference on COMmunication Systems & NETworkS (COMSNETS)*. IEEE, 2021, pp. 572–580.

[12] H. Tabassum, E. Hossain, A. Ogundipe, and D.I. Kim, "Wireless-powered cellular networks: Key challenges and solution techniques," *IEEE Commun. Mag.*, vol. 53, no. 6, pp. 63–71, 2015.

[13] J. Ugwu, K.C. Odo, C.P. Ohanu, J. García, and R. Georgious, "Comprehensive review of renewable energy communication modeling for smart systems," *Energies*, vol. 16, no. 1, p. 409, 2022.

[14] M.A. Ullah, R. Keshavarz, M. Abolhasan, J. Lipman, K.P. Esselle, and N. Shariati, "A review on antenna technologies for ambient rf energy harvesting and wireless power transfer: Designs, challenges and applications," *IEEE Access*, vol. 10, pp. 17 231–17 267, 2022, doi: 10.1109/ACCESS.2022.3149276.

[15] A.A. Nasir, X. Zhou, S. Durrani, and R.A. Kennedy, "Relaying protocols for wireless energy harvesting and information processing," *IEEE Trans. Wirel. Commun.*, vol. 12, no. 7, pp. 3622–3636, 2013.

[16] U. Urosevic, "New solutions for increasing energy efficiency in massive iot," *Signal Image Video Process.*, vol. 16, no. 7, pp. 1861–1868, 2022.

10

*Bull. Pol. Acad. Sci. Tech. Sci.*, vol. 71, no. 5, p. e146620, 2023

[17] S. Manzoor, Y. Yin, Y. Gao, X. Hei, and W. Cheng, "A systematic study of ieee 802.11 dcf network optimization from theory to testbed," *IEEE Access*, vol. 8, pp. 154 114–154 132, 2020.

[18] R. Zhang and C.K. Ho, "Mimo broadcasting for simultaneous wireless information and power transfer," *IEEE Trans. Wireless Commun.*, vol. 12, no. 5, pp. 1989–2001, 2013.

[19] M.M. Salim, H.A. Elsayed, M.S. Abdalzaher, and M.M. Fouda, "Rf energy harvesting effectiveness in relay-based d2d communication," in *2023 International Conference on Computer Science, Information Technology and Engineering (ICCoSITE)*. IEEE, 2023, pp. 342–347.

[20] I. Krikidis, "Simultaneous information and energy transfer in large-scale networks with/without relaying," *IEEE Trans. Commun.*, vol. 62, no. 3, pp. 900–912, 2014.

[21] J. Singh, R. Kaur, and D. Singh, "Energy harvesting in wireless sensor networks: A taxonomic survey," *Int. J. Energy Res.*, vol. 45, no. 1, pp. 118–140, 2021.

[22] K. Huang and V.K. Lau, "Enabling wireless power transfer in cellular networks: Architecture, modeling and deployment," *IEEE Trans. Wirel. Commun.*, vol. 13, no. 2, pp. 902–912, 2014.

[23] T.X. Doan, T.M. Hoang, T.Q. Duong, and H.Q. Ngo, "Energy harvesting-based d2d communications in the presence of interference and ambient rf sources," *IEEE Access*, vol. 5, pp. 5224–5234, 2017.

[24] D.-T. Do and M.-S. Van Nguyen, "Device-to-device transmission modes in noma network with and without wireless power transfer," *Comput. Commun.*, vol. 139, pp. 67–77, 2019.

[25] N.T. Van, T.T. Duy, T. Hanh, and V.N.Q. Bao, "Outage analysis of energy-harvesting based multihop cognitive relay networks with multiple primary receivers and multiple power beacons," in *2017 International Symposium on Antennas and Propagation (ISAP)*. IEEE, 2017, pp. 1–2.

[26] T.D. Hieu, T.T. Duy, and S.G. Choi, "Performance enhancement for harvest-to-transmit cognitive multi-hop networks with best path selection method under presence of eavesdropper," in *2018 20th International Conference on Advanced Communication Technology (ICACT)*. IEEE, 2018, pp. 323–328.

[27] S. Manzoor, Z. Chen, Y. Gao, X. Hei, and W. Cheng, "Towards qos-aware load balancing for high density software defined wi-fi networks," *IEEE Access*, vol. 8, pp. 117 623–117 638, 2020.

[28] J. Mitola, "Cognitive radio for flexible mobile multimedia communications," in *1999 IEEE International Workshop on Mobile Multimedia Communications (MoMuC'99)*. IEEE, 1999, pp. 3–10.

[29] M.A. Hossain, R. Md Noor, S.R. Azzuhri, M.R. Z'aba, I. Ahmedy, K.-L.A. Yau, and C. Chembe, "Spectrum sensing challenges & their solutions in cognitive radio based vehicular networks," *Int. J. Commun. Syst.*, vol. 34, no. 7, p. e4748, 2021.

[30] A. Kumar and K. Kumar, "Multiple access schemes for cognitive radio networks: A survey," *Phys. Commun.*, vol. 38, p. 100953, 2020.

[31] T.N. Nguyen, T.H.Q. Minh, P.T. Tran, M. Voznak, T.T. Duy, T.-L. Nguyen, and P.T. Tin, "Performance enhancement for energy harvesting based two-way relay protocols in wireless ad-hoc networks with partial and full relay selection methods," *Ad Hoc Netw.*, vol. 84, pp. 178–187, 2019.

[32] T.T. Duy, T.Q. Duong, D.B. da Costa, V.N.Q. Bao, and M. Elkashlan, "Proactive relay selection with joint impact of hardware impairment and co-channel interference," *IEEE Trans. Commun.*, vol. 63, no. 5, pp. 1594–1606, 2015.

[33] A. Bilal, S. Latif, S.A. Ghauri, O.-Y. Song, A.A. Abbasi, and T. Karamat, "Modified heuristic computational techniques for the resource optimization in cognitive radio networks (crns)," *Electronics*, vol. 12, no. 4, p. 973, 2023.

[34] E. Bjornson, M. Matthaiou, and M. Debbah, "A new look at dual-hop relaying: Performance limits with hardware impairments," *IEEE Trans. Commun.*, vol. 61, no. 11, pp. 4512–4525, 2013.

[35] H.D. Hung, T.T. Duy, and M. Voznak, "Secrecy outage performance of multi-hop leach networks using power beacon aided cooperative jamming with jammer selection methods," *AEU-Int. J. Electron. Commun.*, vol. 124, p. 153357, 2020.

[36] P. Minh Nam, T. Trung Duy, P. Van Ca, P. Ngoc Son, and N. Hoang An, "Outage performance of power beacon-aided multi-hop cooperative cognitive radio protocol under constraint of interference and hardware noises," *Electronics*, vol. 9, no. 6, p. 1054, 2020.

[37] N.C. Minh, *et al.*, "Reliability-security analysis for harvest-to-jam based multi-hop cluster mimo networks using cooperative jamming methods under impact of hardware impairments," *EAI Endorsed Trans. Ind. Netw. Intell. Syst.*, vol. 8, no. 28, pp. e5–e5, 2021.

[38] T.T. Duy and H.-Y. Kong, "Performance analysis of incremental amplify-and-forward relaying protocols with nth best partial relay selection under interference constraint," *Wirel. Pers. Commun.*, vol. 71, pp. 2741–2757, 2013.

[39] I. Hammerstrom and A. Wittneben, "On the optimal power allocation for nonregenerative ofdm relay links," in *2006 IEEE International Conference on Communications*, vol. 10. IEEE, 2006, pp. 4463–4468.

[40] T. Van Nguyen, T.-N. Do, V.N.Q. Bao, D.B. da Costa, and B. An, "On the performance of multihop cognitive wireless powered d2d communications in wsns," *IEEE Trans. Veh. Technol.*, vol. 69, no. 3, pp. 2684–2699, 2020.

[41] P.K. Sharma and P.K. Upadhyay, "Cognitive relaying with transceiver hardware impairments under interference constraints," *IEEE Commun. Lett.*, vol. 20, no. 4, pp. 820–823, 2016.

[42] G. Liu, F.R. Yu, H. Ji, V.C. Leung, and X. Li, "In-band full-duplex relaying for 5g cellular networks with wireless virtualization," *IEEE Network*, vol. 29, no. 6, pp. 54–61, 2015.

[43] I. Krikidis, J. Thompson, S. McLaughlin, and N. Goertz, "Amplify-and-forward with partial relay selection," *IEEE Commun. Lett.*, vol. 12, no. 4, pp. 235–237, 2008.

[44] K. Tourki, K.A. Qaraqe, and M.-S. Alouini, "Outage analysis for underlay cognitive networks using incremental regenerative relaying," *IEEE Trans. Veh. Technol.*, vol. 62, no. 2, pp. 721–734, 2012.

[45] A. Bletsas, A. Lippnian, and D.P. Reed, "A simple distributed method for relay selection in cooperative diversity wireless networks, based on reciprocity and channel measurements," in *2005 IEEE 61st Vehicular Technology Conference*, vol. 3. IEEE, 2005, pp. 1484–1488.

[46] K. Tourki, H.-C. Yang, and M.-S. Alouini, "Accurate outage analysis of incremental decode-and-forward opportunistic relaying," *IEEE Trans. Wirel. Commun.*, vol. 10, no. 4, pp. 1021–1025, 2011.

[47] C. Zhang, J. Ge, J. Li, F. Gong, Y. Ji, and M.A. Farah, "Energy efficiency and spectral efficiency tradeoff for asymmetric two-way af relaying with statistical csi," *IEEE Trans. Veh. Technol.*, vol. 65, no. 4, pp. 2833–2839, 2015.

[48] J. Choi, "Joint rate and power allocation for noma with statistical csi," *IEEE Trans. Commun.*, vol. 65, no. 10, pp. 4519–4528, 2017.